

On Gamow-Teller strength distributions for $\beta\beta$ -decaying nuclei within continuum-QRPA

S.Yu. Igashov,^{1,*} Vadim Rodin,² Amand Faessler,² and M.H. Urin³

¹*National Nuclear Research University "MEPhI", 115409 Moscow, Russia*

²*Institute für Theoretische Physik der Universität Tübingen, D-72076 Tübingen, Germany*

³*National Research Nuclear University "MEPhI", 115409 Moscow, Russia*

(Dated: November 19, 2019)

An isospin-selfconsistent pn-continuum-QRPA approach is formulated and applied to describe the Gamow-Teller strength distributions for $\beta\beta$ -decaying open-shell nuclei. The calculation results obtained for the pairs of nuclei $^{76}\text{Ge-Se}$, $^{100}\text{Mo-Ru}$, $^{116}\text{Cd-Sn}$, and $^{130}\text{Te-Xe}$ are compared with available experimental data.

PACS numbers: 23.40.-s, 23.40.Bw 23.40.Hc, 21.60.-n,

Keywords: Continuum-random-phase-approximation, Nuclear matrix elements, Double beta decay

I. INTRODUCTION

Description of weak interaction processes in nuclei is often a challenge for nuclear structure models. Numerous calculations of the nuclear double beta ($\beta\beta$) decay amplitudes well illustrate this statement (see, e.g., Refs. [1]). Uncertainties in theoretical calculations of the Gamow-Teller (GT) two-neutrino $\beta\beta$ ($2\nu\beta\beta$) decay amplitude $M_{GT}^{2\nu}$ have stimulated experimental studies of the $\text{GT}(\mp)$ strengths for the transitions to the intermediate 1^+ states virtually excited in the decay process (see, e.g. Refs. [2]-[4]).

As a double charge-exchange process, $2\nu(0\nu)\beta\beta$ -decay is enhanced by nucleon pairing which is due to the singlet part of the particle-particle (p-p) interaction. The discrete quasiboson version of the quasiparticle RPA (pn-dQRPA) which accounts for the nucleon pairing is usually applied to calculate the $\beta\beta$ -decay amplitudes in open-shell nuclei [1]. In spite of differences in the model parametrization of the nuclear mean field and the residual interaction in the particle-hole (p-h) and p-p channels, all pn-dQRPA calculations reveal marked sensitivity of the amplitude $M_{GT}^{2\nu}$ to the ratio g_{pp} of the triplet to singlet p-p interaction strengths. Physical reasons for such a general feature of all calculations were analyzed in Ref. [5], and the sensitivity was shown to reflect violation of the Wigner spin-isospin SU(4) symmetry in nuclei. An identity transformation of the amplitude into the sum of two terms was used in Ref. [5]. One term, which is due to p-p interaction only, depends linearly on g_{pp} and vanishes at $g_{pp} = 1$ where the SU(4)-symmetry is restored in the p-p sector of a model Hamiltonian. The second term is a smoother function of g_{pp} at $g_{pp} \sim 1$, but exhibits a quadratic dependence on the strength of the mean-field spin-orbit term, which is the main source of breaking of the spin-isospin SU(4)-symmetry in nuclei.

Understanding of general properties of the amplitude $M_{GT}^{2\nu}$ helps to improve the reliability of evaluation of the $\beta\beta$ -decay amplitudes. For a quantitative analysis, we use here an isospin-selfconsistent pn-continuum-QRPA (pn-cQRPA) approach, which was initially proposed in Ref. [6] to describe different strength distributions in single-open-shell nuclei. In the reference the full basis of the single-particle (s-p) states was used in the p-h channel along with the Landau-Migdal forces, while the nucleon pairing was described within the simplest version of the BCS-model based on a discrete s-p basis. A rather old version of the phenomenological isoscalar nuclear mean field (including the spin-orbit term) was used in Refs. [5, 6], as well. A further development of the pn-cQRPA approach applied to description of the $\beta\beta$ -decay matrix elements has been given in Ref. [7]. In this reference realistic (zero-range) forces have also been used in the p-p channel to describe the nucleon pairing within the BCS model realized on a rather large discrete+quasidiscrete s-p basis.

In the present work along with the detailed formulation of the pn-cQRPA approach we use a modern version of the phenomenological isoscalar mean field (including the spin-orbit term) deduced in Ref. [8] from the isospin-selfconsistent analysis of experimental single-particle spectra in double-closed-shell nuclei. The last version of the approach and some applications to the GT observables are briefly described in Ref. [9].

The paper organized as follows. In Sect. 2 starting from the coordinate representation of the pn-dQRPA equations, we formulate a pn-cQRPA approach. The expressions for different type strength functions are also given. A realistic

*Electronic address: igashov@theor.mephi.ru

model Hamiltonian and the calculation scheme are described in Sect. 3. In Sect. 4 the results of pn-cQRPA calculations of the GT^\mp strength functions and $M_{GT}^{2\nu}$ amplitudes for the number of nuclei are presented and compared with the available experimental data. Conclusions are drawn in Sect. 5.

II. VERSIONS OF THE PN-QRPA: DISCRETE AND CONTINUUM

A. pn-dQRPA equations in the coordinate representation

The first step towards formulation of a pn-cQRPA approach is transformation of the pn-dQRPA equations to the coordinate representation (see also Refs. [6, 7, 9]). The energies ω_s and wave functions $|s, J^\pi M\rangle$ of the states in the isobaric (odd-odd) nucleus are usually obtained within the quasiboson version of the pn-dQRPA as a solution of a system of homogeneous equations for the forward and backward amplitudes X_s^{JLS} and Y_s^{JLS} related to β^\mp charge-exchange excitations of an even-even parent nucleus. Here, J and M are the total angular momentum and its projection and $\pi = (-1)^L$ is the parity of the intermediate states ($L = 0, 1, 2 \dots$ and $S = 0, 1$ are the transferred orbital momentum and spin, respectively).

The pn-dQRPA eigenenergy solutions ω_s are related to the excitation energies $E_{x,s}^{(\mp)}$ measured from the ground-state energy $E_0(Z \pm 1, N \mp 1)$ of the corresponding daughter nuclei as:

$$\omega_s^{(\mp)} = \omega_s \pm (\mu_p - \mu_n) = E_{x,s}^{(\mp)} + Q_b^{(\mp)}. \quad (1)$$

Here, $\mu_{p(n)}$ is the chemical potential for the proton (neutron) subsystem found from the known BCS equations, $Q_b^{(\mp)} = \mathcal{E}_b(Z, N) - \mathcal{E}_b(Z \pm 1, N \mp 1)$ are the total binding-energy differences, $\omega_s^{(\mp)}$ are the excitation energies measured from $E_0(Z, N) - \sum_a m_a = -\mathcal{E}_b(Z, N)$ (m_a is the nucleon mass). The energies $\omega_s^{(\mp)}$ are usually described by a model Hamiltonian.

For definiteness, we consider further excitations in the β^- channel. The amplitudes $X_{s,\pi\nu}^{JLS}$ and $Y_{s,\pi\nu}^{JLS}$ are based on the discrete s-p levels π and ν for protons and neutrons, respectively (each set π and ν contains the s.p. quantum numbers n_r, l, j). The excitations in the β^+ -channel are described within the pn-dQRPA by the same equations with substitution $p \leftrightarrow n$ ($\pi \leftrightarrow \nu$).

Following Ref. [6], we transform the system of equations for the amplitudes X and Y into the coordinate representation. Transformation is performed in terms of the four-component radial transition density $r^{-2}\varrho_{K,s}^{JLS}(r)$ defined as follows:

$$\begin{aligned} \varrho_{K,s}^{JLSM}(\mathbf{r}) &= \frac{1}{r^2} \varrho_{K,s}^{JLS}(r) T_{JLSM}(\mathbf{n}), \quad \varrho_{K,s}^{JLS}(r) = \sum_{\pi\nu} \varrho_{K,s,\pi\nu}^{JLS} \chi_{\pi\nu}^{JLS}(r), \\ \begin{pmatrix} \varrho_{1,\pi\nu} \\ \varrho_{2,\pi\nu} \\ \varrho_{3,\pi\nu} \\ \varrho_{4,\pi\nu} \end{pmatrix} &= \begin{pmatrix} u_\pi v_\nu X_{\pi\nu} + v_\pi u_\nu Y_{\pi\nu} \\ u_\pi v_\nu Y_{\pi\nu} + v_\pi u_\nu X_{\pi\nu} \\ u_\pi u_\nu X_{\pi\nu} - v_\pi v_\nu Y_{\pi\nu} \\ u_\pi u_\nu Y_{\pi\nu} - v_\pi v_\nu X_{\pi\nu} \end{pmatrix}. \end{aligned} \quad (2)$$

where u, v are the coefficients of Bogolyubov transformation; $\chi_{\pi\nu}^{JLS}(r) = t_{(\pi)(\nu)}^{JLS} \chi_\pi(r) \chi_\nu(r)$ with $\sqrt{2J+1} t_{(\pi)(\nu)}^{JLS} = \langle (\pi) || T_{JLS} || (\nu) \rangle$ being the reduced matrix element of the spin-angular tensor $T_{JLSM}(\mathbf{n} \equiv \mathbf{r}/r)$; $(\pi) = j_\pi, l_\pi$ ($(\nu) = j_\nu, l_\nu$) and $r^{-1}\chi_\pi(r)$ ($r^{-1}\chi_\nu(r)$), being the s-p proton (neutron) quantum numbers and radial wave functions, respectively. Hereafter we shall sometimes omit the superscript “ JLS ” and/or the subscript “ s ” when it does not lead to a confusion.

According to the definition (2), the elements $\varrho_1, \varrho_2, \varrho_3, \varrho_4$ can be called the particle-hole, hole-particle, particle-particle and hole-hole components of the transition density, respectively. In particular, the transition matrix element to a state $|s, J^\pi M\rangle$ corresponding to a probing particle-hole operator

$$\hat{V}_{JLSM}^{(-)} = \sum_a V_L(r_a) T_{JLSM}(\mathbf{n}_a) \tau_a^{(-)} \quad (3)$$

is determined by the element ϱ_1 as:

$$\langle s, J^\pi M | \hat{V}_{JLSM}^{(-)} | 0 \rangle = \int \varrho_{1,s}^{JLS}(r) V_L(r) dr. \quad (4)$$

Assuming the residual interaction F_K^S in the p-h ($K = 1, 2$) and p-p ($K = 3, 4$) channels to be momentum-independent, one can represent the system of homogeneous pn-dQRPA equations (primarily written for the amplitudes X and Y) in the equivalent form:

$$\varrho_{K,s}^{JLS}(r) = \sum_{K'} \int A_{KK'}^{JLS}(r, r', \omega = \omega_s) F_{K'}^S(r', r'') \varrho_{K',s}^{JLS}(r'') dr' dr''. \quad (5)$$

Here, $(rr')^{-1}F_K^S(r, r')$ is the radial part of the residual interaction, the 4×4 matrix $(rr')^{-2}A_{KK'}(r, r', \omega)$ is the radial part of the free two-quasiparticle propagator hereafter taken diagonal on L, S (the so-called "symmetric" approximation [6]):

$$\begin{aligned} A_{KK'}(r_1, r_2, \omega) &= \sum_{\pi\nu} \chi_{\pi\nu}(r_1) \chi_{\pi\nu}(r_2) A_{KK',\pi\nu}(\omega), \quad A_{KK',\pi\nu} = A_{K'K,\pi\nu}, \quad (6) \\ A_{11,\pi\nu} &= \frac{u_\pi^2 v_\nu^2}{\omega - E_{\pi\nu}} - \frac{u_\nu^2 v_\pi^2}{\omega + E_{\pi\nu}}, \quad A_{33,\pi\nu} = \frac{u_\pi^2 u_\nu^2}{\omega - E_{\pi\nu}} - \frac{v_\nu^2 v_\pi^2}{\omega + E_{\pi\nu}}, \\ A_{12,\pi\nu} &= -A_{34,\pi\nu} = u_\pi v_\pi v_\nu u_\nu \left(\frac{1}{\omega - E_{\pi\nu}} - \frac{1}{\omega + E_{\pi\nu}} \right), \\ A_{13,\pi\nu} &= u_\nu v_\nu \left(\frac{u_\pi^2}{\omega - E_{\pi\nu}} + \frac{v_\pi^2}{\omega + E_{\pi\nu}} \right), \quad A_{14,\pi\nu} = -u_\pi v_\pi \left(\frac{v_\nu^2}{\omega - E_{\pi\nu}} + \frac{u_\nu^2}{\omega + E_{\pi\nu}} \right), \end{aligned}$$

$$A_{22,\pi\nu}(\omega) = A_{11,\pi\nu}(-\omega), \quad A_{44,\pi\nu}(\omega) = A_{33,\pi\nu}(-\omega), \quad A_{23\pi\nu}(\omega) = A_{14,\pi\nu}(-\omega), \quad A_{24,\pi\nu}(\omega) = A_{13,\pi\nu}(-\omega),$$

with $E_{\pi\nu} = E_\pi + E_\nu$, where $E_\pi (E_\nu)$ is the proton (neutron) quasiparticle energy. Excitations in the β^+ -channel are described within the pn-dQRPA by Eqs. (5),(6) with the substitution $p \leftrightarrow n$ ($\pi \leftrightarrow \nu$). The relationship $A_{KK',\nu\pi}(\omega) = A_{KK',\pi\nu}(-\omega)$, which follows from Eq. (6), allows one to reduce pn-QRPA description of excitations in the β^+ -channel to pn-QRPA description of excitations in the β^- -channel. In particular, because of equalities $A_{11,\nu\pi}(\omega) = A_{11,\pi\nu}(-\omega) = A_{22,\pi\nu}(\omega)$, the transition matrix element to the state $|s, J^\pi M\rangle$ corresponding to a probing operator $\hat{V}_{JLSM}^{(+)}$ (given by Eq. (3) with substitution $\tau^{(-)} \rightarrow \tau^{(+)}$) is determined by the transition-density element ϱ_2 : $\langle s, J^\pi M | \hat{V}_{JLSM}^{(+)} | 0 \rangle = \int \varrho_{2,s}^{JLS}(r) V_L(r) dr$. In such a description the operator $\hat{V}_{JLSM}^{(+)}$ can be considered as the hole-particle one.

B. QRPA effective operators and strength functions

The next step towards taking the s-p continuum into account is consideration of the effective two-quasiparticle propagator (two-quasiparticle Green function) $\tilde{A}_{KK'}(r, r', \omega)$, which satisfies a Bethe-Salpeter-type equation [7]:

$$\tilde{A}_{KK'}^{JLS}(r, r', \omega) = A_{KK'}^{JLS}(r, r', \omega) + \sum_{K''} \int A_{KK''}^{JLS}(r, r_1, \omega) F_{K''}^S(r_1, r_2) \tilde{A}_{K''K'}^{JLS}(r_2, r', \omega) dr_1 dr_2. \quad (7)$$

Here, the current energy ω is related to the excitation energy of daughter nuclei: $\omega^{(\mp)} = \omega \pm (\mu_p - \mu_n)$ (compare with Eq.(1)). The spectral decomposition of the effective propagator contains all the necessary information about the pn-QRPA solutions:

$$\tilde{A}_{11}^{JLS}(r_1, r_2, \omega) = \sum_s \frac{\varrho_{1,s}^{JLS}(r_1) \varrho_{1,s}^{JLS}(r_2)}{\omega - \omega_s + i0} - \sum_s \frac{\varrho_{2,s}^{JLS}(r_1) \varrho_{2,s}^{JLS}(r_2)}{\omega + \omega_s - i0}, \quad (8)$$

$$\tilde{A}_{22}^{JLS}(r_1, r_2, \omega) = \tilde{A}_{11}^{JLS}(r_1, r_2, -\omega), \quad (9)$$

$$\tilde{A}_{12}^{JLS}(r_1, r_2, \omega) = \sum_s \frac{\varrho_{1,s}^{JLS}(r_1) \varrho_{2,s}^{JLS}(r_2)}{\omega - \omega_s + i0} - \sum_s \frac{\varrho_{2,s}^{JLS}(r_1) \varrho_{1,s}^{JLS}(r_2)}{\omega + \omega_s - i0}. \quad (10)$$

In practical applications of the pn-QRPA method it is more convenient to use four-component effective fields $\tilde{V}_{K[I]}(r, \omega)$ corresponding to the probing operator $V(r)$ acting in the particle-hole ($I = 1$) or hole-particle ($I = 2$) channels. The effective fields are defined as follows:

$$\int \tilde{A}_{KI}(r, r', \omega) V(r') dr' = \sum_{K'} \int A_{KK'}(r, r', \omega) \tilde{V}_{K'[I]}(r', \omega) dr'. \quad (11)$$

The system of equations for the effective operators follows from Eqs. (7),(11):

$$\tilde{V}_{K[I]}^{JLS}(r, \omega) = V_L(r)\delta_{KI} + \sum_{K'} \int F_K^S(r, r') A_{KK'}^{JLS}(r', r'', \omega) \tilde{V}_{K'[I]}^{JLS}(r'', \omega) dr' dr''. \quad (12)$$

Similar equations are given in Ref. [10], where they are obtained by the methods of the Migdal's finite Fermi-system theory.

By definition, the strength functions corresponding to the probing operators of Eq. (3) are:

$$S_{JLS}^{(\mp)}(\omega) = \sum_s \left| \langle s, J^\pi \| \hat{V}_{JLS}^{(\mp)} \| 0 \rangle \right|^2 \delta(\omega - \omega_s). \quad (13)$$

Making use of the spectral expansion Eq. (9), one can express the strength functions in terms of the two-quasiparticle effective propagator, or in equivalent terms of the corresponding effective fields:

$$\begin{aligned} S_{JLS}^{(-)}(\omega) &= -\frac{1}{\pi}(2J+1) \text{Im} \int V_L(r_1) \tilde{A}_{11}^{JLS}(r_1, r_2, \omega) V(r_2) dr_1 dr_2 = \\ &= -\frac{1}{\pi}(2J+1) \text{Im} \sum_K \int V_L(r_1) A_{1K}^{JLS}(r_1, r_2, \omega) \tilde{V}_{K[1]}^{JLS}(r_2, \omega) dr_1 dr_2. \end{aligned} \quad (14)$$

$$\begin{aligned} S_{JLS}^{(+)}(\omega) &= -\frac{1}{\pi}(2J+1) \text{Im} \int V_L(r_1) \tilde{A}_{22}^{JLS}(r_1, r_2, \omega) V(r_2) dr_1 dr_2 = \\ &= -\frac{1}{\pi} \text{Im}(2J+1) \sum_K \int V_L(r_1) A_{2K}^{JLS}(r_1, r_2, \omega) \tilde{V}_{K[2]}^{JLS}(r_2, \omega) dr_1 dr_2. \end{aligned} \quad (15)$$

Within the pn-QRPA description of the $\beta\beta$ -decay amplitudes it is useful to consider a “non-diagonal” strength function [7]:

$$S_{JLS}^{(--)}(\omega) = \sum_s \langle 0' \| \hat{V}_{JLS}^{(-)} \| s, J^\pi \rangle \langle s, J^\pi \| \hat{V}_{JLS}^{(-)} \| 0 \rangle \delta(\omega - \omega_s), \quad (16)$$

where $|0'\rangle$ is the ground state wave function of the final nucleus. Identifying the pn-QRPA vacuum $|0'\rangle$ with that for $|0\rangle$, one gets the following expressions:

$$\begin{aligned} S_{JLS}^{(--)}(\omega) &= -\frac{1}{\pi}(2J+1) \text{Im} \int V_L(r_1) \tilde{A}_{21}^{(JLS)}(r_1, r_2, \omega) V_L(r_2) dr_1 dr_2 = \\ &= -\frac{1}{\pi}(2J+1) \text{Im} \sum_K \int V_L(r_1) A_{2K}^{(JLS)}(r_1, r_2, \omega) \tilde{V}_{K[1]}^{JLS}(r_2, \omega) dr_1 dr_2. \end{aligned} \quad (17)$$

Bearing in mind applications of the method to describing the GT^\pm strength functions and $2\nu\beta\beta$ -decay amplitude $M_{GT}^{2\nu}$, in this paper we limit concrete consideration by the case $(JLS) = (101)$ and use for this case the probing GT operators $\hat{G}_M^\mp = \sum_a \sigma_M(a) \tau_a^{(\mp)}$. Here σ_M are the Pauli spherical matrices, the radial part of the corresponding external field of Eq.(3) is $V_{L=0}(r) = \sqrt{4\pi}$. The integrated strength functions $S_{GT}^{(\mp)}$ satisfy the Ikeda sum rule equal $3(N-Z)$.

C. $2\nu\beta\beta$ -decay amplitude

The nuclear GT^- amplitude for the $2\nu\beta\beta$ -decay into the ground state $|0'\rangle$ of the final nucleus $(Z+2, N-2)$ is given by the expression

$$M_{GT}^{2\nu} = \sum_s \bar{\omega}_s^{-1} \langle 0' \| \hat{G}^- \| s, 1^+ \rangle \langle s, 1^+ \| \hat{G}^- \| 0 \rangle, \quad (18)$$

where $\bar{\omega}_s = E_s - \frac{1}{2}(E_0 + E_{0'}) = E_{x,s} + \frac{1}{2}(Q_b^{(-)} + Q^{(+)'})_b$. To calculate $M_{GT}^{2\nu}$ within the pn-QRPA, the vacua $|0\rangle$ and $|0'\rangle$ should be identified. As a result of such identification, one has $\bar{\omega}_s = \frac{1}{2}(\omega_s^{(-)} + \omega^{(+)'})_s \approx \omega_s$ in accordance

with Eq.(1). Therefore, the amplitude (16) can be directly expressed in terms of the “non-diagonal” GT^- strength function of Eqs. (14),(15):

$$M_{GT}^{2\nu} = \int \omega^{-1} S_{GT}^{(-)}(\omega) d\omega. \quad (19)$$

An alternative expression for $M_{GT}^{2\nu}$ is obtained in terms of the “non-diagonal” static polarizability [7]:

$$M_{GT}^{2\nu} = -3\sqrt{\pi} \sum_i \int A_{2i}^{101}(r, r', \omega = 0) \tilde{V}_{i[1]}^{(-)}(r', \omega = 0) dr dr'. \quad (20)$$

As mentioned in Introduction , the amplitude of Eq. (16) can be decomposed in a model-independent way into two terms [5]:

$$M_{GT}^{2\nu} = M'_{GT} + M''_{GT}, \quad M''_{GT} = \frac{EWSR_{GT}^{(-)}}{\bar{\omega}_{GTR}^2}, \quad (21)$$

where $\bar{\omega}_{GTR}$ is the energy of the GT^- giant resonance (GTR), and $EWSR_{GT}^{(-)} = \int \omega S_{GT}^{(-)}(\omega) d\omega$ is the “non-diagonal” energy-weighted sum rule. This sum rule, which is determined by the p-p interaction only, is mainly responsible for the sensitivity of the amplitude $M_{GT}^{2\nu}$ to the ratio g_{pp} of the triplet to singlet strength of the p-p interaction. The sum rule $EWSR_{GT}^{(-)}$ depends linearly on g_{pp} and vanishes at $g_{pp} = 1$ where the SU(4) symmetry is restored in the p-p sector of a model Hamiltonian. The term M'_{GT} in Eq. (19) is a smoother function of g_{pp} at $g_{pp} \sim 1$, but exhibits a quadratic dependence of the strength of the mean-field spin-orbit term, which is the main source of violation of the spin-isospin SU(4)-symmetry in nuclei.

D. Exact treatment of the single-particle continuum in the particle-hole channel

The above given coordinate representation of the pn-dQRPA equations is fully equivalent to the version usually formulated in terms of the X and Y amplitudes, provided a discrete basis of s-p states is used. However, the use of the coordinate representation allows us to exactly take into account the s-p continuum in the p-h channel and, therefore, to formulate a version of the continuum-pn-QRPA (pn-cQRPA) (see also Refs. [6, 7, 9]). Within this version the pairing problem is solved on a basis of bound and quasibound proton and neutron s-p states. To take the s-p continuum into account , the following transformations in Eq. (6) is performed: (i) the Bogolyubov coefficients v_λ , u_λ and the quasiparticle energies E_λ are approximated by their non-pairing values $v_\lambda=0$, $u_\lambda = 1$ and $E_\lambda = \epsilon_\lambda - \mu$ for those s-p states, which lie far above the chemical potential (i.e., $(\epsilon_\lambda - \mu) \gg \Delta$); (ii) the radial s-p Green function $g_{(\lambda)}(r, r', \epsilon) = \sum_{\epsilon_\lambda} (\epsilon - \epsilon_\lambda + i0)^{-1} \chi_\lambda(r) \chi_\lambda(r')$ is used to explicitly perform the sum over s-p states in the continuum ($\lambda = \epsilon_\lambda, (\lambda); (\lambda) = j_\lambda, l_\lambda$). As a result, we get from Eq. (6) the following representation of the properly transformed

free two-quasiparticle propagator:

$$\begin{aligned}
A_{11}(r_1, r_2, \omega) &= \sum_{\nu <, \pi <} \frac{v_\nu^2 u_\pi^2 \chi_{\pi\nu}(r_1) \chi_{\pi\nu}(r_2)}{\omega - E_{\pi\nu}} + \sum_{\nu <, (\pi)} t_{(\pi)(\nu)}^2 \chi_\nu(r_1) \chi_\nu(r_2) v_\nu^2 g'_{(\pi)}(r_1, r_2, \mu_\pi + \omega - E_\nu) \\
&\quad + \{p \leftrightarrow n, \pi \leftrightarrow \nu, \omega \leftrightarrow -\omega\}, \tag{22} \\
A_{12}(r_1, r_2, \omega) &= \sum_{\nu <, \pi <} u_\nu v_\nu u_\pi v_\pi \chi_{\pi\nu}(r_1) \chi_{\pi\nu}(r_2) \left(\frac{1}{\omega - E_{\pi\nu}} - \frac{1}{\omega + E_{\pi\nu}} \right), \\
A_{13}(r_1, r_2, \omega) &= \sum_{\pi <, \nu} \chi_{\pi\nu}(r_1) \chi_{\pi\nu}(r_2) u_\nu v_\nu \left(\frac{u_\pi^2}{\omega - E_{\pi\nu}} + \frac{v_\pi^2}{\omega + E_{\pi\nu}} \right) \\
&\quad + \sum_{(\pi), \nu} t_{(\pi)(\nu)}^2 \chi_\nu(r_1) \chi_\nu(r_2) u_\nu v_\nu g'_{(\pi)}(r_1, r_2, \omega + \mu_p - E_\nu), \\
A_{14}(r_1, r_2, \omega) &= - \sum_{\pi, \nu <} \chi_{\pi\nu}(r_1) \chi_{\pi\nu}(r_2) u_\pi v_\pi \left(\frac{v_\nu^2}{\omega - E_{\pi\nu}} + \frac{u_\nu^2}{\omega + E_{\pi\nu}} \right) \\
&\quad + \sum_{\pi <, (\nu)} t_{(\pi)(\nu)}^2 \chi_\pi(r_1) \chi_\pi(r_2) u_\pi v_\pi g'_{(\nu)}(r_1, r_2, \mu_n - \omega - E_\pi), \\
A_{33}(r_1, r_2, \omega) &= \sum_{\pi <, \nu <} \chi_{\pi\nu}(r_1) \chi_{\pi\nu}(r_2) \left(\frac{u_\pi^2 u_\nu^2}{\omega - E_{\pi\nu}} - \frac{v_\pi^2 v_\nu^2}{\omega + E_{\pi\nu}} \right) \\
&\quad + \sum_{\pi <, (\nu)} t_{(\pi)(\nu)}^2 \chi_\pi(r_1) \chi_\pi(r_2) u_\pi^2 g'_{(\nu)}(r_1, r_2, \omega - E_\pi + \mu_n) \\
&\quad + \sum_{\nu <, (\pi)} t_{(\pi)(\nu)}^2 \chi_\nu(r_1) \chi_\nu(r_2) u_\nu^2 g'_{(\pi)}(r_1, r_2, \omega - E_\nu + \mu_p).
\end{aligned}$$

Here, $\pi < (\nu <)$ means $\pi \leq \pi_{max}$ ($\nu \leq \nu_{max}$), where π_{max} (ν_{max}) is taken so that $E_{\pi_{max}} = \varepsilon_{\pi_{max}} - \mu_p$ ($E_{\nu_{max}} = \varepsilon_{\nu_{max}} - \mu_n$) with an acceptable accuracy, and the projected radial s-p Green function is:

$$g'_{(\lambda)}(r_1, r_2, \varepsilon) = g_{(\lambda)}(r_1, r_2, \varepsilon) - \sum_{\lambda <} \frac{\chi_\lambda(r_1) \chi_\lambda(r_2)}{\varepsilon - \varepsilon_\lambda}. \tag{23}$$

The first sum in this expression is running over all the s-p states and can be calculated via a product of the regular and irregular solutions of the corresponding s-p Schrödinger equation. Such a representation of $g_{(\lambda)}(r_1, r_2, \varepsilon)$ has been used in Ref. [11] to formulate the very first version of the continuum-RPA. Other $A_{KK'}$ (r, r', ω) components in Eq. (22) are obtained in the same way, as it is done in Eq. (6). Thus, Eq. (22) together with Eqs. (23) and (12) realize a version of the pn-cQRPA method. As applied to description of the Fermi and GT strength distributions in single-open-shell nuclei, the method was used in Ref. [6]. This pn-cQRPA approach has been applied to description of the $\beta\beta$ -decay matrix elements in Ref. [7].

Within the pn-cQRPA the spectral decomposition of Eq. (9) remains valid, provided the continuum-states $|s\rangle$ (normalized to the δ -function of the energy) are taken into consideration. These states are characterized, in particular, by the particle-hole (hole-particle) energy-dependent transition densities which determine the strength functions as follows:

$$S_{JLS}^{(\mp)}(\omega) = (2J+1) \left| \int V_L(r) \varrho_{JLS}^{(\mp)}(r, \omega) dr \right|^2. \tag{24}$$

These transition densities can be expressed in terms of the effective fields corresponding to the probing operators of Eq. (3) and their partners. Supposing the p-h interaction is of zero range (with the intensities $F_1^S = F_2^S = 2F^S$), one gets from Eqs. (12)-(15) the expressions:

$$\varrho_{JLS}^{(-)}(r, \omega) = -\frac{1}{\pi} \text{Im} \frac{(2J+1)^{1/2} \tilde{V}_{1[1]}^{(JLS)}(r, \omega)}{2F^S \sqrt{S_{JLS}^{(-)}(\omega)}}, \quad \varrho_{JLS}^{(+)}(r, \omega) = -\frac{1}{\pi} \text{Im} \frac{(2J+1)^{1/2} \tilde{V}_{2[2]}^{(JLS)}(r, \omega)}{2F^S \sqrt{S_{JLS}^{(+)}(\omega)}}. \tag{25}$$

The intensities F^S may be radial-dependent.

III. CALCULATION OF THE GT STRENGTH FUNCTIONS AND THE $2\nu\beta\beta$ -DECAY AMPLITUDES WITHIN THE PN-CQRPA

A. Model Hamiltonian: interactions in the particle-hole and particle-particle channels

For quantitative realization of the relationships given in the preceding Section, we specify the nuclear Hamiltonian. We adopt here the realistic model Hamiltonian, which is an extended version of that used in Refs. [6, 7]. The Hamiltonian consists of the mean field and residual interactions. The partially selfconsistent mean field is described in the Subsect. B. Here, we specify interactions in the p-h and p-p channels, \hat{H}_{p-h} and \hat{H}_{p-p} , respectively. As \hat{H}_{p-h} , we use the Landau-Migdal forces in the charge-exchange channels:

$$\hat{H}_{p-h} = 2 \sum_{a>b} (F^0 + F^1 \boldsymbol{\sigma}_a \boldsymbol{\sigma}_b) \tau_a^{(-)} \tau_b^{(+)} \delta(\mathbf{r}_a - \mathbf{r}_b) + h.c., \quad (26)$$

where the intensities F^S of the non-spin-flip ($S = 0$) and spin-flip ($S = 1$) parts of this interaction are the phenomenological parameters. We choose the zero-range p-p interaction in both the neutral (pairing) and charge-exchange channels:

$$\hat{H}_{p-p} = -\frac{1}{2} \sum_{\substack{JLSM \\ \lambda\lambda'\lambda_1\lambda'_1}} G^S(\lambda\lambda'\lambda_1\lambda'_1)_{JLS} \left(P_{\lambda\lambda'}^{JM} \right)^\dagger P_{\lambda_1\lambda'_1}^{JM}, \quad (27)$$

where G^S are the intensities of the p-p interaction in the $S = 0, 1$ channels, and (differently from the below-given equations) the sums over s-p states include the neutron and proton states, $(\lambda\lambda'\lambda_1\lambda'_1)_{JLS} = \int \chi_{\lambda,\lambda'}^{JLS}(r) \chi_{\lambda_1,\lambda'_1}^{JLS}(r) \frac{dr}{r^2}$. The annihilation operator P^{JM} for a nucleon pair is given, as follows:

$$P_{\lambda\lambda'}^{JM} = \sum_{m,m'} \langle JM | j_\lambda m, j_{\lambda'} m' \rangle a_{\lambda' m'} a_{\lambda m}, \quad (28)$$

where $a_{\lambda m}$ ($a_{\lambda m}^\dagger$) is the annihilation (creation) operator of a nucleon in the state with the quantum numbers λm (m is the projection of the particle angular momentum), $\langle JM | j_\lambda m, j_{\lambda'} m' \rangle$ is the Clebsch-Gordan coefficient. The p-h interaction of Eq. (26) can also be expressed in terms of the operators a^\dagger and a :

$$\hat{H}_{p-h} = 2 \sum_{\substack{JLSM \\ \pi\nu\pi'\nu'}} F^S(\pi\nu\pi'\nu')_{JLS} \left(A_{\pi\nu}^{JM} \right)^\dagger A_{\pi'\nu'}^{JM} + \left(\pi \leftrightarrow \nu \right), \quad (29)$$

where the creation p-h operator A^\dagger is given as follows:

$$\left(A_{\pi\nu}^{JM} \right)^\dagger = \sum_{m_\pi, m_\nu} \langle JM | j_\pi m_\pi, j_\nu - m_\nu \rangle (-1)^{j_\nu - m_\nu} a_{\pi m_\pi}^\dagger a_{\nu m_\nu}. \quad (30)$$

In solution of the pairing problem we simplify the p-p interaction (27) for the 0^+ neutral channel, using the ‘‘diagonal’’ approximation: $\lambda = \lambda'$, $\lambda_1 = \lambda'_1$. The nucleon pairing is described with the use of the Bogolyubov transformation in terms of the quasiparticle creation (annihilation) operators $\alpha_{\lambda m}^\dagger$, $\alpha_{\lambda m}$ (see, e.g., Ref. [12]). As a result, the following model Hamiltonian is obtained to describe charge-exchange excitations within the pn-QRPA:

$$\hat{H} = \hat{H}_{0,n} + \hat{H}_{0,p} + \mu_n \hat{N} + \mu_p \hat{Z} + \hat{H}_{p-h} + \hat{H}_{p-p}, \quad \hat{H}_0 = \sum_{\lambda m} E_\lambda \alpha_{\lambda m}^\dagger \alpha_{\lambda m}. \quad (31)$$

Here, $E_\lambda = \sqrt{(\varepsilon_\lambda - \mu)^2 + \Delta_\lambda^2}$ is the quasiparticle energy. The chemical potentials μ and the energy-gap parameters Δ_λ are determined by solving the BCS-model equations for even and odd subsystems (with the number of nucleons $N(\text{even})$ and $N(\text{odd})$ nucleons, respectively):

$$N(\text{even}) = \sum_\lambda (2j_\lambda + 1) v_\lambda^2, \quad \Delta_\lambda(\text{even}) = G^0 \sum_{\lambda'} (2j_{\lambda'} + 1) (\lambda \lambda \lambda' \lambda')_{000} \frac{\Delta_{\lambda'}}{2E_{\lambda'}}, \quad (32)$$

$$N(\text{odd}) = \sum_{\lambda \neq \lambda_0} (2j_\lambda + 1)v_\lambda^2 + (2j_{\lambda_0} - 1)v_{\lambda_0}^2 + 1, \quad (33)$$

$$\Delta_\lambda(\text{odd}) = G^0 \left\{ \sum_{\lambda' \neq \lambda_0} (2j_{\lambda'} + 1)(\lambda\lambda\lambda'\lambda')_{000} \frac{\Delta_{\lambda'}}{2E_{\lambda'}} + (2j_{\lambda_0} - 1)(\lambda\lambda\lambda_0\lambda_0)_{000} \frac{\Delta_{\lambda_0}}{2E_{\lambda_0}} \right\}. \quad (34)$$

Here, λ_0 labels the level occupied by the odd quasiparticle. Following the standard procedure, we introduce different strengths G_n^0 and G_p^0 of the p-p interaction in the 0^+ pairing channels to reproduce the experimental pairing energies. The latter are expressed via the ground-state binding energies calculated within the BCS model:

$$- \mathcal{E}_b(\text{even}) = \sum_{\lambda} (2j_\lambda + 1)v_\lambda^2(\mu - E_\lambda), \quad (35)$$

$$- \mathcal{E}_b(\text{odd}) = \sum_{\lambda \neq \lambda_0} (2j_\lambda + 1)v_\lambda^2(\mu - E_\lambda) + (2j_{\lambda_0} - 1)v_{\lambda_0}^2(\mu - E_{\lambda_0}) + \varepsilon_{\lambda_0}. \quad (36)$$

The level λ_0 is chosen from the minimum of the calculated $-\mathcal{E}_b$, and/or accordingly to the quantum numbers of the odd-nucleus ground state. To roughly correct for double counting in evaluation of the total energy, we properly modify Eqs. (35),(36): $(\mu - E_\lambda) \rightarrow (\mu - E_\lambda - \frac{1}{2}U_{\lambda\lambda})$; $\varepsilon_{\lambda_0} \rightarrow \varepsilon_{\lambda_0} - \frac{1}{2}U_{\lambda_0\lambda_0}$. Here $U_{\lambda\lambda}$ is the diagonal matrix element of the nuclear mean field (Subsect. B).

The explicit expressions for the p-h and p-p interactions in terms of the quasiparticle (pn)-pair creation and annihilation operators are:

$$\hat{H}_{p-h} = 2 \sum_{\substack{JLSM \\ \pi\nu\pi'\nu'}} F^S(\pi\nu\pi'\nu')_{JLS} \left(Q_{\pi\nu}^{JM} \right)^\dagger Q_{\pi'\nu'}^{JM} + \left(p \leftrightarrow n, \pi \leftrightarrow \nu \right), \quad (37)$$

$$\hat{H}_{p-p} = - \sum_{\substack{JLSM \\ \pi\nu\pi'\nu'}} G^S(\pi\nu\pi'\nu')_{JLS} \left(\mathcal{P}_{\pi\nu}^{JM} \right)^\dagger \mathcal{P}_{\pi'\nu'}^{JM}, \quad (38)$$

where

$$Q_{\pi\nu}^{JM} = u_\pi v_\nu \mathcal{A}_{\pi\nu}^{JM} + v_\pi u_\nu \left(\mathcal{A}_{\pi\nu}^{J\widetilde{M}} \right)^\dagger, \quad \mathcal{P}_{\pi\nu}^{JM} = u_\pi u_\nu \mathcal{A}_{\pi\nu}^{JM} - v_\pi v_\nu \left(\mathcal{A}_{\pi\nu}^{J\widetilde{M}} \right)^\dagger, \quad (39)$$

$$\mathcal{A}_{\pi\nu}^{JM} = \sum_{mm'} \langle JM | j_\pi m, j_\nu m' \rangle \alpha_{\nu m'} \alpha_{\pi m}, \quad \mathcal{A}_{\pi\nu}^{J\widetilde{M}} = (-1)^{J-M} \mathcal{A}_{\pi\nu}^{J-M}. \quad (40)$$

The forward and backward amplitudes X and Y are defined by the corresponding matrix elements $X_{s,\pi\nu}^{JLS} = \langle s, J^\pi | (\mathcal{A}_{\pi\nu}^{JM})^\dagger | 0 \rangle$ and $Y_{s,\pi\nu}^{JLS} = \langle s, J^\pi | \mathcal{A}_{\pi\nu}^{J\widetilde{M}} | 0 \rangle$. The system of equations for these amplitudes can be explicitly derived using the model Hamiltonian of Eqs. (31), (37)-(40). Having transformed this system to the form given by Eqs. (2),(5),(6), one can relate the interaction $F_K^S(r, r')$, entering the basic pn-QRPA Eqs. (5), (12), to the model-Hamiltonian zero-range interactions of Eqs. (37)-(40):

$$F_K^S(r, r') = F_K^S \frac{\delta(r - r')}{r r'}, \quad F_{K=1,2}^S = 2F^S, \quad F_{K=3,4}^S = -G^S. \quad (41)$$

Thus, within the model under consideration there are four phenomenological interaction strength parameters F^S , G^S ($S = 0, 1$) which will be specified below.

B. Model Hamiltonian: the mean field and selfconsistency conditions

The nuclear mean field consists of the isoscalar (central and spin-orbit), isovector and Coulomb parts:

$$U(x) = U_0(x) + U_1(x) + U_C(x), \quad U_0(x) = U_0(r) + U_{SO}(r)\mathbf{l}\sigma, \quad (42)$$

$$U_1(x) = \frac{1}{2}v(r)\tau^{(3)}, \quad U_C(x) = \frac{1}{2}(1 - \tau^{(3)})U_C(r), \quad (43)$$

where $v(r)$ is the symmetry potential. Within the model the mean-field isoscalar part is treated phenomenologically (that seems well justified for description of isovector excitations), while the isovector and Coulomb parts are calculated selfconsistently.

The realistic phenomenological isoscalar mean field is parametrized as follows:

$$U_0(r) = -U_0 f_{WS}(r, R, a), \quad U_{SO}(r) = U_{SO} \frac{1}{r} \frac{df_{WS}}{dr}, \quad (44)$$

where $f_{WS} = (1 + \exp(\frac{r-R}{a}))^{-1}$ is the Woods-Saxon function with the radius $R = r_0 A^{1/3}$ and the diffuseness parameter a . To avoid spurious violation of the isospin symmetry caused by the mean-field isovector part, the latter is calculated using the isospin-selfconsistency condition [6]. This condition relates the symmetry potential to the isovector nuclear density (the neutron-excess density) via the isovector (non-spin-flip) part of the p-h interaction (26):

$$v(r) = 2F^0(n^n(r) - n^p(r)). \quad (45)$$

Here, the neutron and proton densities are calculated with taking into account nucleon pairing:

$$n_{even}(r) = \frac{1}{4\pi r^2} \sum_{\lambda} (2j_{\lambda} + 1) v_{\lambda}^2 \chi_{\lambda}^2(r), \quad (46)$$

$$n_{odd}(r) = \frac{1}{4\pi r^2} \left\{ \sum_{\lambda \neq \lambda_0} (2j_{\lambda} + 1) v_{\lambda}^2 \chi_{\lambda}^2(r) + \left[(2j_{\lambda_0} - 1) v_{\lambda_0}^2 + 1 \right] \chi_{\lambda_0}^2(r) \right\}. \quad (47)$$

The mean Coulomb field $U_C(r)$ is also calculated selfconsistently within the Hartree approximation via the proton density (46),(47). Thus, the above-described mean field is a partially selfconsistent one. Nevertheless, the isospin symmetry of the model Hamiltonian is slightly violated due to approximate description of the nucleon pairing (the use of the “diagonal” approximation, truncation of the s-p basis, different values of the G_n^0 and G_p^0 pairing strengths). These approximations can affect the quality of the calculated Fermi excitations, but they seem to be of rather minor importance for calculations of the GT excitations considered in this work.

C. Choice of model parameters and the calculation scheme

Recently, a partially selfconsistent mean field has been adopted to describe experimental single-particle spectra in the doubly-closed-shell nuclei ^{48}Ca , ^{132}Sn , ^{208}Pb [8]. As a starting point, the fully phenomenological mean field of Ref. [13] was used. The deduced strength parameters U_0 , U_{SO} , $F^0 = C f'$ ($C = 300 \text{ MeV} \cdot \text{fm}^3$) and also the diffuseness parameter a reveal a weak A-dependence (the value $r_0 = 1.27 \text{ fm}$ is taken the same for all nuclei [13]). This point allows us to use for the nuclei under consideration the properly interpolated values of the model parameters mentioned above (Table 1). Then, the partially selfconsistent mean field (42)-(47) and the corresponding s-p level scheme are calculated to get a basis for the BCS solution of the nucleon pairing problem accordingly to Eqs. (32)-(34). This problem is solved consistently with calculation of the symmetry potential and mean Coulomb field by making use of the neutron and proton densities (46),(47) and a set of the pairing strength parameters G_{α}^0 . The latter are then fitted to reproduce the experimental pairing energies \mathcal{E}_{pair} [14]:

$$\mathcal{E}_{pair}(N) = \pm \left\{ \frac{1}{8} \mathcal{E}_b(N+2) - \frac{1}{2} \mathcal{E}_b(N+1) + \frac{3}{4} \mathcal{E}_b(N) - \frac{1}{2} \mathcal{E}_b(N-1) + \frac{1}{8} \mathcal{E}_b(N-2) \right\} \quad (48)$$

with “+” or “-” related to $N(\text{even})$ or $N(\text{odd})$, respectively. As \mathcal{E}_b in this expression (the corresponding experimental values are taken from Ref. [15]), we use the properly modified ground-state energies of Eqs. (35),(36). For the subsystems having $N_c \pm 2$ nucleons (N_c is a magic number) we use a simplified expression for the pairing energy:

$$\mathcal{E}_{pair}(N_c \pm 2) = -\frac{1}{4} \mathcal{E}_b(N_c \pm 1) + \frac{3}{4} \mathcal{E}_b(N_c \pm 2) - \frac{3}{4} \mathcal{E}_b(N_c \pm 3) + \frac{1}{4} \mathcal{E}_b(N_c \pm 4). \quad (49)$$

The parameters $G_{n,p}^0 = C g_{n,p}^0$, fitted as described above, are listed in Table 1. To reduce an artificial violation of the isospin symmetry, caused by the use of only discrete (quasidiscrete) s-p states in description of the pairing problem,

we use the same number of these states N_{d+qd} for the proton and neutron subsystems. The N_{d+qd} values for the nuclei under consideration are also given in Table 1. The energy and the radial wave function of a quasibound state λ are found using the representation of the radial Green function, which is valid inside the nucleus at the energies close to the quasibound state energy:

$$g_{(\lambda)}(r, r', \varepsilon) = \frac{\chi_{\lambda}(r)\chi_{\lambda}(r')}{\varepsilon - \varepsilon_{\lambda} + \frac{i}{2}\Gamma_{\lambda}}, \quad (50)$$

where Γ_{λ} is the quasibound-state escape width.

After the consistent solution of the pairing problem, we turn to evaluation of the GT^{\pm} strength functions and amplitudes $M_{GT}^{2\nu}$ within the present pn-cQRPA approach. To calculate these quantities in accordance with Eqs. (12), (14), (15) and Eqs. (17), (19), (21), respectively one has to choose the strengths $F^1 = Cg'$ and G^1 (or $g_{pp} = 2G^1/(G_n^0 + G_p^0)$) of the spin-flip parts of the p-h and p-p interactions. Using in evaluation of the GT^- strength function the realistic value $g_{pp} = 1$, we find the strength g' to reproduce in calculations the experimental GTR energy. The fitted strength values are listed in Table 2. These values are weakly dependent on the variation of g_{pp} in a vicinity of the point $g_{pp} = 1$. Having chosen g' , the amplitudes $M_{GT}^{2\nu}$, their components M'_{GT} and M''_{GT} are calculated as functions of g_{pp} for the pairs of nuclei $^{76}\text{Ge-Se}$, $^{100}\text{Mo-Ru}$, $^{116}\text{Cd-Sn}$ and $^{130}\text{Te-Xe}$. Since the ^{116}Sn nucleus has the filled proton shell, in evaluation of the amplitude $M_{GT}^{2\nu}$ for the pair $^{116}\text{Cd-Sn}$ we identify the vacuum $|0'\rangle$ with that for $|0\rangle$. The strengths $g_{pp} \sim 1$, which allow us to reproduce in calculations the experimental $M_{GT}^{2\nu}$ values, are also listed in Table 2. These strengths are further used to evaluate the $2\nu\beta\beta$ -decay GT reduced strength function $S_{GT}^{2\nu}(\omega) = \omega^{-1}S_{GT}^{(-)}(\omega)/M_{GT}^{2\nu}$ (normalized to unity) and the corresponding reduced running sum $r_{GT}^{2\nu}(\omega) = \int^{\omega} S_{GT}^{2\nu}(\omega)d\omega$ (goes to unity at large ω). Along with the above-mentioned decomposition these quantities show how the amplitudes $M_{GT}^{2\nu}$ are formed from the partial contribution of 1^+ states in the intermediate nucleus. Finally, the fitted g' and g_{pp} values are used to calculate the GT^{\mp} strength functions. To compare with the experimental GT^- strength distribution it is convenient to consider the reduced running sum $r_{GT}^{(-)}(\omega) = \int^{\omega} S_{GT}^{(-)}(\omega)d\omega/S_{GTR}^{(-)}$, where $S_{GTR}^{(-)}$ is the GT^- strength of the GTR. We show also the (non-reduced) running sum $R_{GT}^{(+)}(\omega) = \int^{\omega} S_{GT}^{(+)}(\omega)d\omega$ for the GT^+ strength in the final nucleus. All the calculations are performed without taking into account the quenching of the total GT strength.

IV. CALCULATION RESULTS

Within the pn-cQRPA approach described in the preceding Sections we calculate the $2\nu\beta\beta$ -decay amplitudes $M_{GT}^{2\nu}$ and the corresponding GT^{\pm} strength functions for the pairs of nuclei $^{76}\text{Ge-Se}$, $^{100}\text{Mo-Ru}$, $^{116}\text{Cd-Sn}$ and $^{130}\text{Te-Xe}$. The results are presented in Figs. 1.-4. Each figure contains: a) the amplitude $M_{GT}^{2\nu}$ and its decomposition in two terms in accordance with Eq. (21) calculated as functions of the strength g_{pp} ; b) the reduced $2\nu\beta\beta$ -decay GT strength function $S_{GT}^{2\nu}(\omega)$ calculated at the g_{pp} value fitted to reproduce in calculations the experimental amplitude $M_{GT}^{2\nu}$ (Table 2.); c) the reduced $2\nu\beta\beta$ -decay running sum $r_{GT}^{2\nu}(\omega)$ calculated at the fitted g_{pp} value; d) the calculated GT^- strength function $S_{GT}^{(-)}(\omega)$ for the initial nucleus, e) and f) the running sums $r_{GT}^{(-)}$ and $R_{GT}^{(+)}$ for the initial and final nuclei, respectively. The results are compared with available experimental data.

The calculated results shown in Figs. 1.a), b), c) - 4.a), b), c) demonstrate how the amplitudes $M_{GT}^{2\nu}$ are formed for the nuclei under consideration. The general features are the almost linear dependence of the component M'_{GT} on the p-p interaction strength g_{pp} and vanishing of these amplitudes at $g_{pp} \approx 1$. Thus, we confirm the conclusion of Ref. [5] (obtained within a simpler model) that the component M'_{GT} is only determined by the p-p residual interaction and goes to zero at $g_{pp} = 1$ where the spin-isospin $\text{SU}(4)$ -symmetry is restored in the p-p sector of this model Hamiltonian¹. As compared with Ref. [5], in our calculations the components M'_{GT} (and, therefore, the amplitudes $M_{GT}^{2\nu}$) are somewhat smaller since the strength of the mean-field spin-orbit term used in our calculations is smaller. Again we confirm the conclusion of Ref. [5] that at $g_{pp} \sim 1$ the component M'_{GT} essentially depends on the spin-orbit term only, which is the main source of $\text{SU}(4)$ -symmetry breaking in nuclei. Details of the formation of the amplitudes $M_{GT}^{2\nu}$ are dependent on the shell-structure of nuclei. As follows from Figs. 2.b), 2.c) and 3.b), 3.c), population of the 1^+ ground state of the intermediate nuclei ^{100}Tc and ^{116}In dominates the formation of the amplitudes $M_{GT}^{2\nu}$ for the pairs $^{100}\text{Mo-Ru}$ and $^{116}\text{Cd-Sn}$, respectively. Within the used calculation scheme the proper GT^- and GT^+ transitions are mainly to the single-quasiparticle $g_{9/2}^n \rightarrow g_{7/2}^p$ and $g_{7/2}^p \rightarrow g_{9/2}^n$ transitions, respectively. For the pairs $^{76}\text{Ge-Se}$ and

¹ In the QRPA calculations using a realistic G-matrix residual interaction [19] this point of crossing zero is shifted to $g_{pp} < 1$ due to the effect of $\text{SU}(4)$ -symmetry breaking by the tensor forces in the residual interaction

TABLE I: The phenomenological mean field parameters, singlet p-h and p-p interaction strengths, and the number of the bound and quasibound s-p states used in calculations.

Nuclei	U_0 , MeV	U_{SO} , MeV·fm ²	a , fm	f'	$g_{0,n}$	$g_{0,p}$	N_{b+qb}
⁷⁶ Ge- ⁷⁶ Se	51.3	34.4	0.60	1.17	0.41	0.32	16
¹⁰⁰ Mo- ¹⁰⁰ Ru	51.5	34.2	0.61	1.13	0.45	0.41	16
¹¹⁶ Cd- ¹¹⁶ Sn	51.6	34.1	0.62	1.06	0.39	0.33	22
¹³⁰ Te- ¹³⁰ Xe	51.7	34.0	0.63	1.09	0.36	0.36	22

¹³⁰Te-Xe the amplitudes $M_{GT}^{2\nu}$ are formed by population of many 1^+ states of the intermediate nuclei ⁷⁶As and ¹³⁰I, respectively (Figs. 1.b), 1.c) and 4.b), 4.c)). It means, in particular, that the intermediate states having a relatively large excitation energy and, therefore, a small $B(GT^+)$ value (like the GTR) can, nevertheless, play essential role in the formation of the amplitude $M_{GT}^{2\nu}$. For this reason, the experimental studies aimed to deduce the corresponding $B(GT^\pm)$ values for the intermediate 1^+ states and then to reconstruct the amplitudes $M_{GT}^{2\nu}$ seem to be sufficient in the case of the approximate single-state dominance. The proper examples are the studies performed for 1^+ states in ¹⁰⁰Tc [17] and ¹¹⁶In [3], but it might not be fully correct in the case of the study of ⁷⁶As [4].

Turning to calculations of the $GT^{(\mp)}$ strength functions, we start from the description of the GTR in the intermediate nuclei ⁷⁶As, ¹⁰⁰Tc, ¹¹⁶Sb, ¹³⁰I. The strength functions $S_{GT}^{(-)}(\omega)$ are shown in Figs. 1.d)-4.d) (similarly to the strength functions shown in Figs. 1.b)-4.b) we add a small imaginary part to the s-p potential while calculating the s-p Green's function in order to make the presentation more visible). Using the experimental data of Refs. [16–18] on charge-exchange reactions, we fit the p-h strength parameter g' to reproduce in calculations the experimental value of the centroid of the GTR energy (Table 2). For A=116 systems we have performed the fitting of the GTR in ¹¹⁶Sb in view of the absence of appropriate experimental data for ¹¹⁶In. However, the value $B(GT^{(-)})=0.26\pm 0.02$ has been deduced in Ref. [2] from the ¹¹⁶Cd(p,n)-reaction with population of the 1^+ ground state in ¹¹⁶In. Within the interval $E_x \leq 3$ MeV the calculated $GT^{(-)}$ -strength distribution in ¹¹⁶In exhibits one 1^+ state, corresponding to the back-spin-flip transition $1g_{7/2}^n \rightarrow 1g_{9/2}^p$ into the 1^+ ground state of ¹¹⁶In, with the value $B(GT^{(-)})=1.05$ (for ¹¹⁶Sn \rightarrow ¹¹⁶Sb this transition is Pauli blocked). Bearing in mind that the low-energy part of the $GT^{(\mp)}$ strength distributions cannot be described in details within any pn-QRPA-based approach (for instance, in view of existence of the quasiparticle-phonon coupling), we compare with experimental data the running sums $r_{GT}^{(-)}(\omega)$, $R_{GT}^{(+)}(\omega)$. The calculated and experimental running sums $r_{GT}^{(-)}$ shown in Figs. 1.d)-4.d), at least qualitatively, agree. With the exception for the running sums $R_{GT}^{(+)}$ for the pairs ⁷⁶Se-⁷⁶As (Fig. 1.f)) and ¹¹⁶Sn-¹¹⁶In (Fig. 3.f)), a reasonable description of the data is found for the $B(GT^+)$ values corresponding to the ground-state to ground-state 1^+ transitions ¹⁰⁰Tc-¹⁰⁰Ru (Fig. 2.f) and ¹¹⁶Sn-¹¹⁶In (Fig. 3.f).

V. CONCLUSIONS

We have given a detailed formulation of a version of the proton-neutron continuum-QRPA approach that makes use of:

- (i) realistic zero-range interactions in the particle-hole and particle-particle channels;
- (ii) a modern version of the phenomenological isospin-self-consistent nuclear mean field;
- (iii) the full basis of the particle-hole excitations, and a rather large basis of the particle-particle ones (with inclusion of several quasi-bound s-p states). Within the approach we have studied “anatomy” of the Gamow-Teller $2\nu\beta\beta$ -decay amplitude for a number of nuclei. The concept of the broken spin-isospin SU(4)-symmetry in nuclei has been made use of in the study of the g_{pp} -sensitivity of $M_{GT}^{2\nu}$. A reasonable description of the Gamow-Teller strength functions in β^\mp -channels for the nuclei in question has been obtained within the approach.

Sensitivity of the calculated observables to realistic variations of the mean field parameters is going to be studied elsewhere.

Acknowledgments

This work of S.Yu.I. and M.H.U. is supported in part by the Russian Foundation for Basic Researches under Contract No. 09-02-00926-a. V.A.R. and A.F. acknowledge support of the Deutsche Forschungsgemeinschaft within the SFB TR27 “Neutrinos and Beyond”.

TABLE II: The phenomenological triplet p-h and p-p interaction strengths. The experimental GTR energies from Refs. [16]-[18] and the amplitudes $M_{GT}^{2\nu}$ from Ref. [20] are also given.

Nuclei	$E_{x,GTR}$, MeV	g'	$M_{GT}^{2\nu}$, MeV $^{-1}$	g_{pp}
^{76}Ge - ^{76}Se	11.13 [16]	0.81	0.14	0.62
^{100}Mo - ^{100}Ru	13.3 [17]	0.92	0.24	0.91
^{116}Cd - ^{116}Sn	10.04 [18]	0.77	0.13	1.07
^{130}Te - ^{130}Xe	13.59 [16]	0.88	0.03	0.99

-
- [1] A. Faessler and F. Šimkovic, J. Phys. G **24**, 2139 (1998); J. Suhonen and O. Civitarese, Phys. Rept. **300**, 123 (1998); S.R. Elliott and P. Vogel, Annu. Rev. Nucl. Part. Sci. **52**, 115 (2002); S. R. Elliott and J. Engel, J. Phys. G **30**, R183 (2004); Frank T. Avignone III, Steven R. Elliott, and Jonathan Engel, Rev. Mod. Phys. **80**, 481 (2008).
- [2] M. Sasano et al., Nucl. Phys. A **788**, 76c (2007).
- [3] S. Rakers et al., Phys. Rev. C **71**, 054313 (2005).
- [4] E.-W. Grewe et al., Phys. Rev. C **78**, 044301 (2008).
- [5] V.A. Rodin, M.H. Urin, and A. Faessler, Nucl. Phys. A **747**, 295 (2005).
- [6] V.A. Rodin and M.H. Urin, Phys. At. Nuclei **66**, 2128 (2003), nucl-th/0201065.
- [7] V. Rodin and A. Faessler, Phys. Rev. C **77**, 025502 (2008).
- [8] S.Yu. Igashov, M.H. Urin, Bull.Rus.Acad.Sci.Phys. **70**, 212 (2006).
- [9] S.Yu. Igashov, V.A. Rodin, M.H. Urin, and A. Faessler, Phys. At. Nucl. **71**, 1267 (2008).
- [10] I.N. Borzov, E.L. Trykov, and S.A. Fayans, Nucl. Phys. A **584**, 335 (1995); I.N. Borzov and S. Goriely, Phys. Rev. C **62**, 035501 (2000).
- [11] S. Shlomo and G.F. Bertsch, Nucl Phys. A **243**, 507 (1975).
- [12] V.G. Soloviev, Theory of Complex Nuclei (Pergamon, Oxford, 1976).
- [13] B.I. Isakov et al., Phys. At. Nucl. **67**, 1856 (2004).
- [14] P. Moeller and R.J. Nix, Nucl. Phys. A **536**, 20 (1992).
- [15] G. Audi, A.H. Wapstra, and C. Thibault, Nucl. Phys. A **729**, 337 (2003).
- [16] R. Madey, B.S. Flanders, B.D. Anderson, A.R. Baldwin, J.W. Watson, S.M. Austin, C.C. Foster, H.V. Klapdor and K. Grotz, Phys. Rev. C **40**, 540 (1989).
- [17] H. Akimune, H. Ejiri, M. Fujiwara, I. Daito, T. Inomata, R. Hazama, A. Tamii, H. Toyokawa, M. Yosoi, Phys. Lett. B **394**, 23 (1997).
- [18] K. Pham et al., Phys. Rev. C **51**, 526 (1995).
- [19] V. A. Rodin, A. Faessler, F. Simkovic and P. Vogel, Nucl. Phys. **A766**, 107 (2006); **A793**, 213(E) (2007); F. Šimkovic, A. Faessler, V.A. Rodin, P. Vogel, and J. Engel, Phys. Rev. C **77**, 045503 (2008); F. Šimkovic, A. Faessler, H. Mütter, V.A. Rodin, and M. Stauf, Phys. Rev. C **79**, 055501 (2009).
- [20] A.S. Barabash, Czech. J. Phys. **50**, 437 (2006), nucl-ex/0602009.

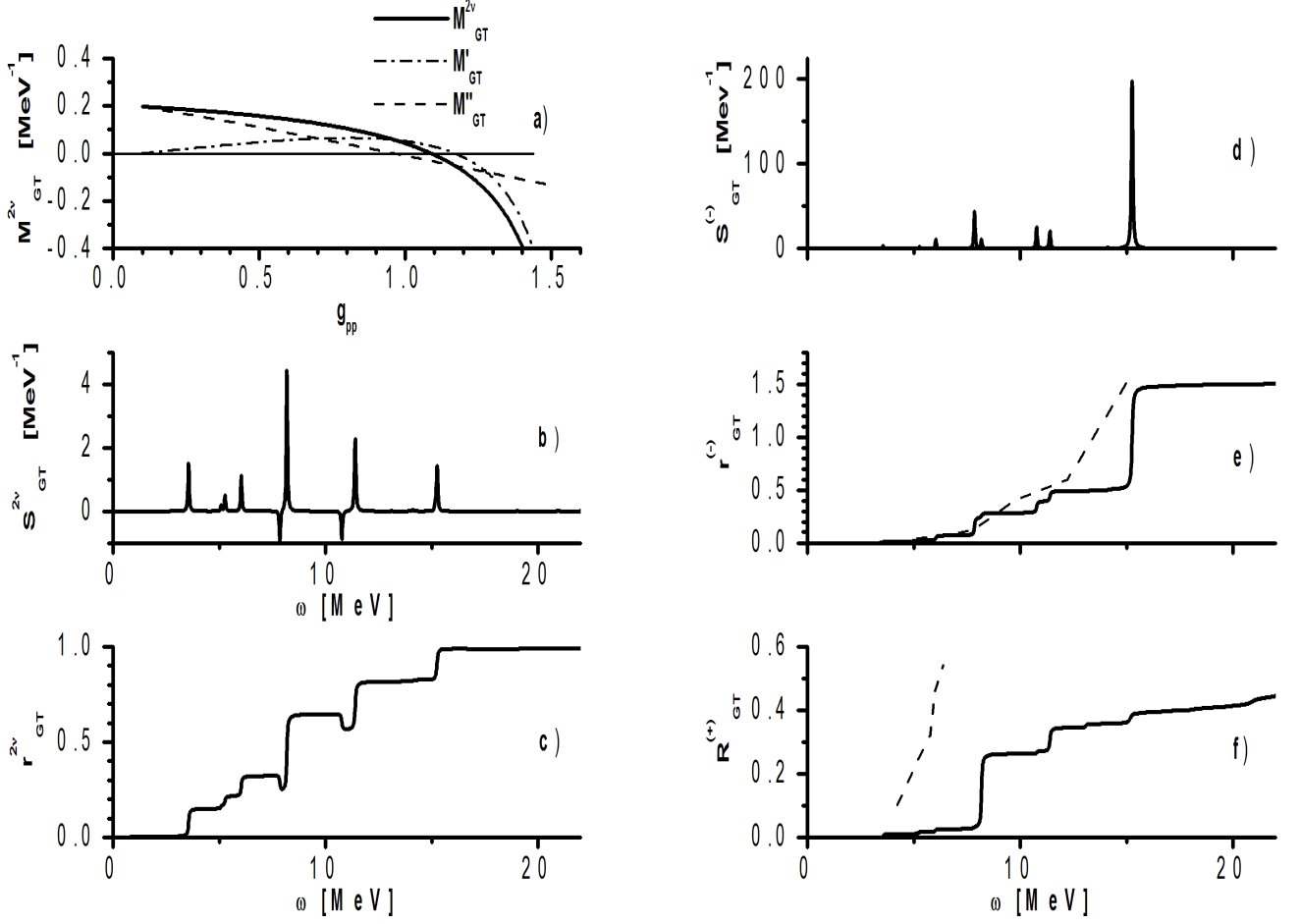


FIG. 1: a) the $2\nu\beta\beta$ -decay GT amplitude $M_{GT}^{2\nu}$ (full line) and their components M_{GT}^{\prime} (dotted-point line), $M_{GT}^{\prime\prime}$ (dotted line) calculated as a function of the strength g_{pp} for the pair $^{76}\text{Ge-Se}$; b) and c) the $2\nu\beta\beta$ -decay reduced GT strength function and running sum, respectively, calculated at the strength g_{pp} from Table 2 for the same pair of nuclei; d) and e) the GT $^{-}$ strength function and reduced running sum, respectively, calculated at the strengths g' and g_{pp} from Table 2 for the pair $^{76}\text{Ge-As}$ (full line), the experimental data (dashed line) are taken from Ref. [16]; f) the GT $^{+}$ running sum calculated at the strengths g' and g_{pp} from Table 2 for the pair $^{76}\text{Se-As}$ (full line), the experimental data (dashed line) are taken from Ref. [4].

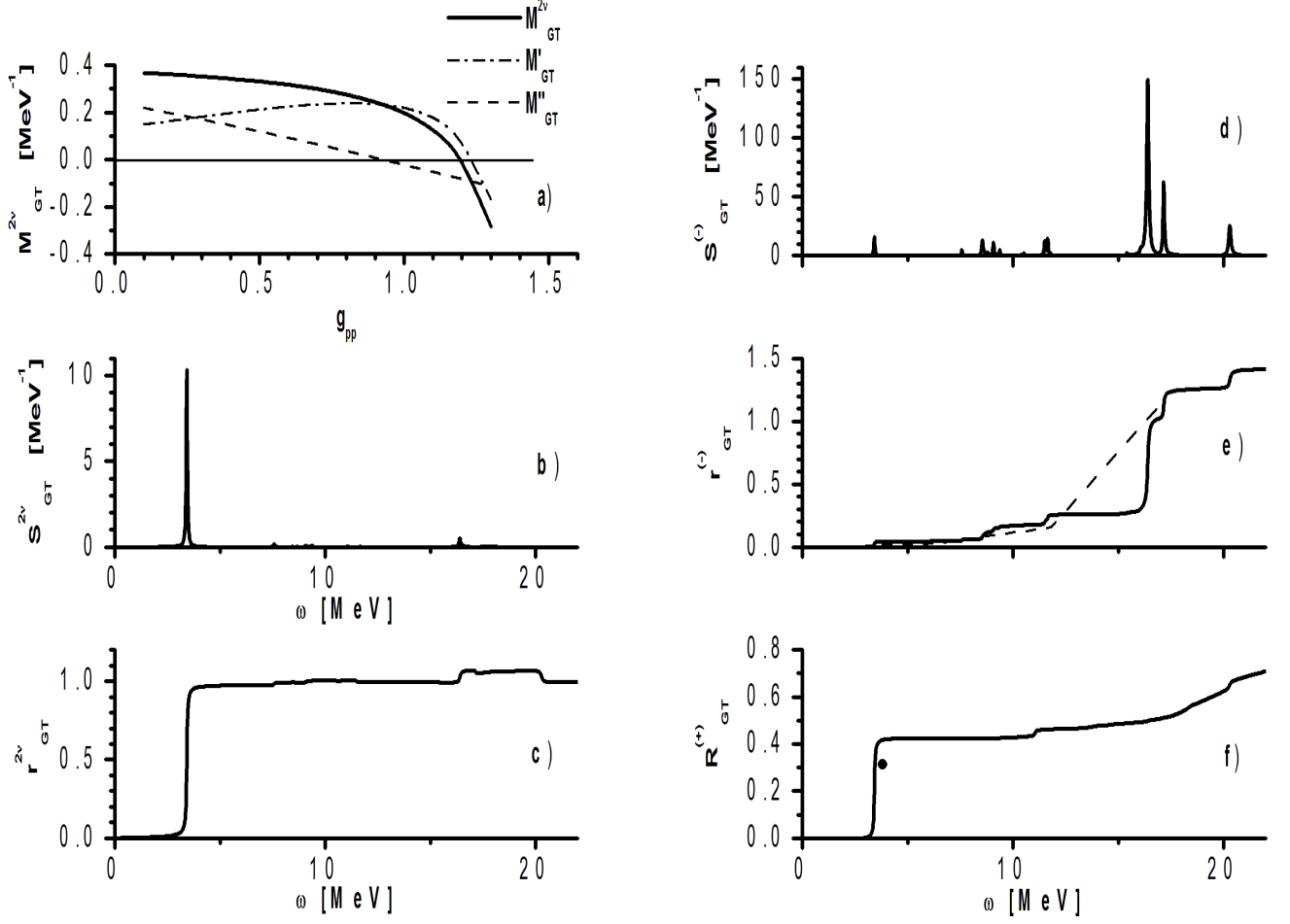


FIG. 2: a)-c) the same as in Figs. 1.a)-1.c) but for the pair $^{100}\text{Mo-Ru}$; d) and e) the same as in Figs. 1.d) and 1.e) but for the pair $^{100}\text{Mo-Tc}$, the experimental data are taken from Ref. [17]; f) the same as in Fig. 1.f) but for the pair $^{100}\text{Ru-Tc}$, the experimental data (noted by the circle) are taken from Ref. [17].

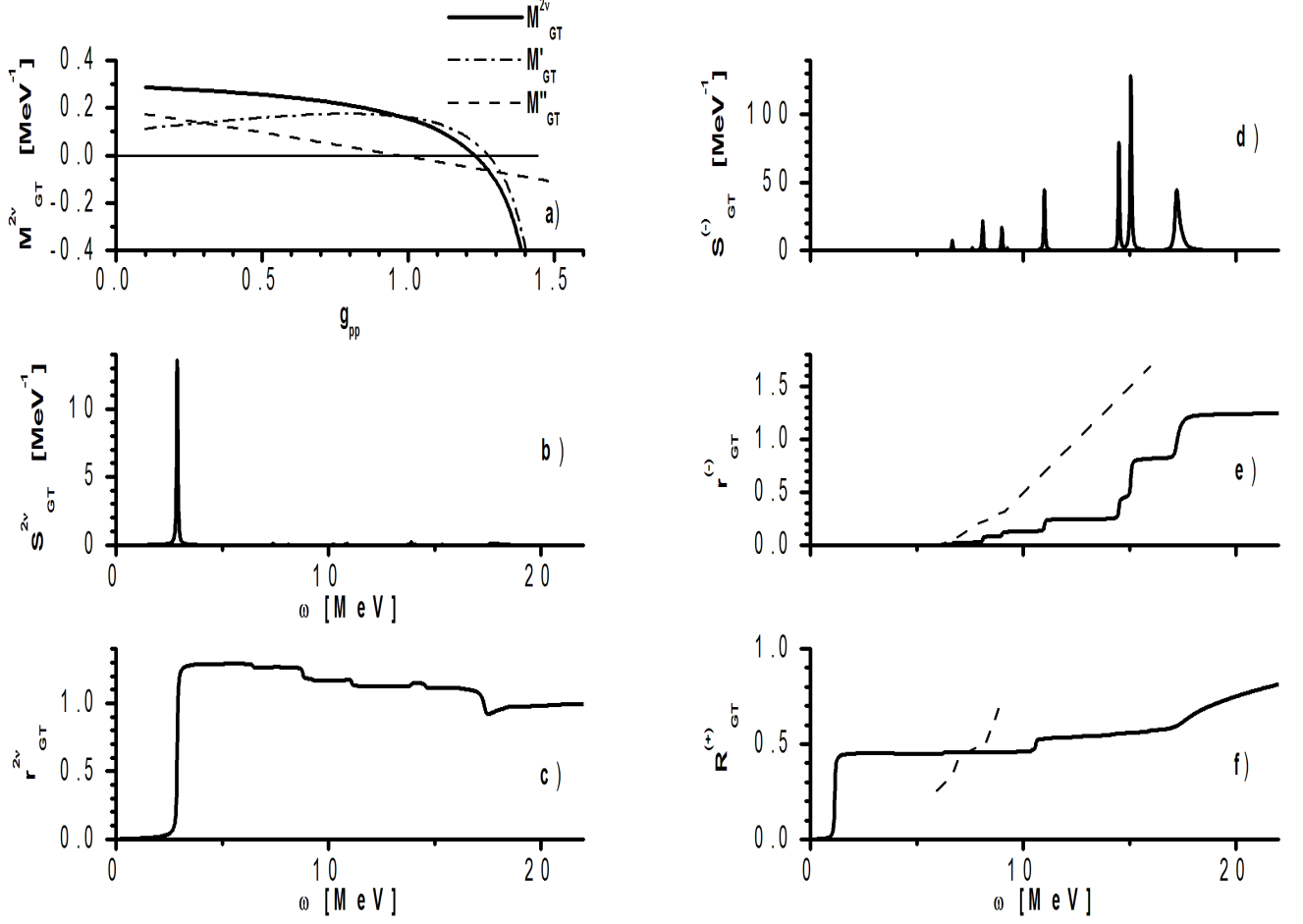


FIG. 3: a)-c) the same as in Figs. 1.a)-1.c) but for the pair $^{116}\text{Cd-Sn}$; d) and e) the same as in Figs. 1.d) and 1.e) but for the pair $^{116}\text{Sn-Sb}$, the experimental data (related to the differential $(^3\text{He,t})$ -reaction cross section at 0°) are taken from Ref. [18]; f) the same as in Fig. 1.f) but for the pair $^{116}\text{Sn-In}$, the experimental data are taken from Ref. [3].

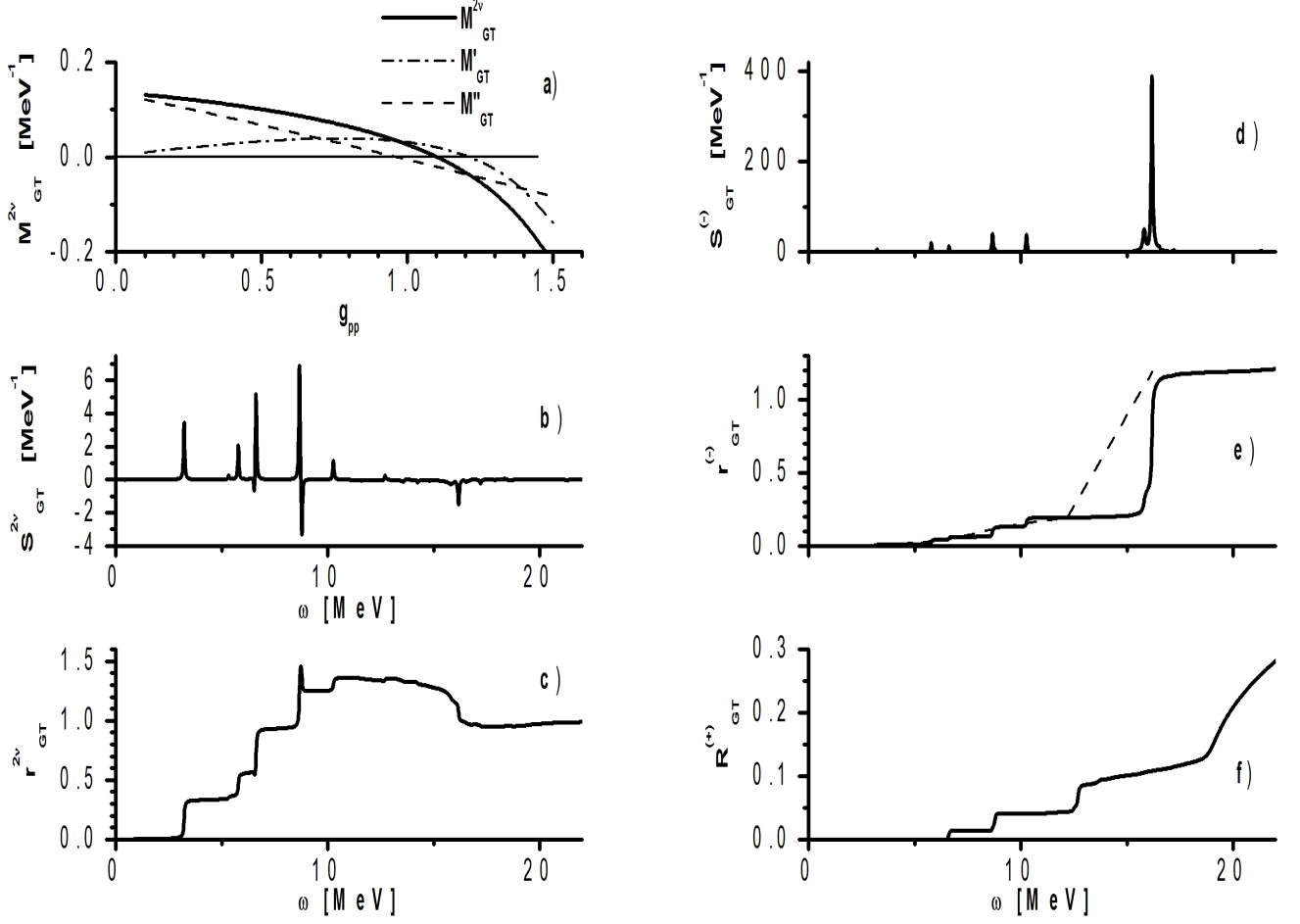


FIG. 4: a)-c) the same as in Figs. 1.a)-1.c) but for the pair $^{130}\text{Te-Xe}$; d) and e) the same as in Figs. 1.d) and 1.e) but for the pair $^{130}\text{Te-I}$, the experimental data are taken from Ref. [16]; f) the same as in Fig. 1.f) but for the pair $^{130}\text{Xe-I}$.